

Third-Order Nonlinear Optical Response of Fullerenes as a Function of the Carbon Cage Size (C₆₀ to C₉₆) at 0.532 μm

Houjin Huang, Gang Gu,[†] and Shihe Yang*

Department of Chemistry, Hong Kong University of Science & Technology,
Clear Water Bay, Kowloon, Hong Kong

Jishi Fu, Ping Yu, and George K. L. Wong

Department of Physics, Hong Kong University of Science & Technology,
Clear Water Bay, Kowloon, Hong Kong

Youwei Du

Laboratory of Solid State Microstructures and Department of Physics, Nanjing University,
Nanjing 210093, P. R. China

Received: August 13, 1997; In Final Form: November 3, 1997[⊗]

We report the results of our degenerate four-wave-mixing measurements (DFWM) on the fullerene series from C₆₀ to C₉₆ dissolved in CS₂. The DFWM measurements were carried out using 70 ps laser pulses at the wavelength of 0.532 μm under the optimized experimental conditions. The second hyperpolarizabilities γ_{1111} of all these fullerenes were determined to be on the order of 10^{-31} – 10^{-30} esu, and overall they increase smoothly with the carbon cage size except for C₇₀ and C₇₈, which show anomalously larger γ_{1111} values than those of their neighboring cage sizes we investigated. The number of π -conjugated electrons, geometrical structure, and resonance enhancement are discussed as possible factors responsible for the observed third-order optical nonlinearities of the fullerenes.

I. Introduction

Soon after its discovery, buckminsterfullerene has received a great deal of research effort devoted to explore its nonlinear optical properties.^{1–26} The expectation that buckminsterfullerene could be a good nonlinear optical material is hinged on its extensive three-dimensional π -electron conjugation for one thing and its quantum dot nature for another.¹ A further desirable characteristic of this all-carbon molecule in comparison with organic or polymer nonlinear optical materials is that no bonds such as C–H or O–H are present, which would otherwise induce absorption and limit their use in nonlinear optics. Indeed, a large nonlinear optical response of buckminsterfullerene C₆₀ was observed by a number of research groups, suggesting that buckminsterfullerene is among the most promising nonlinear optical (NLO) materials.^{1,3,9,11,13,16,21} It is important to recognize, however, that because the third-order nonlinear optical responses are very sensitive to many experimental factors such as the measurement techniques adopted, the incident laser power, and even the sample preparation method employed, the direct comparison of results on nonlinear optical properties of C₆₀ obtained from different groups by different techniques has proven to be rather difficult.^{24,26}

While there is definitely a need to resolve the controversies among different measurements, an equally important issue of general interest is how the nonlinear optical properties of fullerenes evolve as a function of the cage size. Ideally, such

measurements should be performed using the same techniques under identical conditions for the sake of comparison of nonlinear optical properties among different fullerenes. Recently, theoretical studies indicate that the reduction in symmetry of higher fullerenes would result in an increase in their third-order polarizabilities.²⁵ It has also been predicted that the second hyperpolarizability of a higher fullerene scales with the third or fourth power of the mass of the all-carbon molecule.^{17,22} However, few experimental data are available regarding the nonlinear optical response of higher fullerenes. Although there has been one optical Kerr effect measurement which is concerned with the third-order optical nonlinearity of C₈₄, the sample purity was not satisfactory.²¹

The advances in higher fullerene separation allowed the extensive fullerene series from C₆₀ to C₁₀₀ to be isolated in good yield and high purity.^{27,28} It is therefore not only necessary but also feasible to study the nonlinear optical response of fullerenes as a function of the carbon cage size. In this work, we report our comparative DFWM investigations on high-purity fullerene series from C₆₀ to C₉₆ in CS₂ solutions. We have already given a preliminary account on the comparison of the nonlinear optical properties between C₉₀ and C₆₀.²⁹ Considering that the second hyperpolarizabilities γ_{1111} of fullerenes measured by different research groups may differ significantly, we carried out careful studies on the concentration dependence and laser power dependence of the nonlinear responses of the fullerene samples to find out the best measurement conditions. Our measurements revealed that the second hyperpolarizabilities of all these fullerenes are in the range 10^{-31} – 10^{-30} esu, and they in general increase with the fullerene cage size with the

* E-mail: chsyang@usthk.ust.hk.

[†] Present address: Laboratory of Solid State Microstructures and Department of Physics, Nanjing University, China.

[⊗] Abstract published in *Advance ACS Abstracts*, December 1, 1997.

exception of only C_{70} and C_{78} , which exhibit higher nonlinear optical response than their neighboring fullerenes under study.

II. Experimental Section

Details of the fullerene sample preparation procedures can be found elsewhere.^{30,31} The soot produced by a standard arc vaporization method was collected and extracted in a Soxhlet extractor using *N,N*-dimethylformamide (DMF, 99.9%, BDH) at its boiling temperature for about 10 h. After removal of the DMF by evaporation, a black powder was obtained. The soluble fraction was dissolved in toluene and injected into an HPLC. A 5PYE column (10 × 250 mm; Cosmosil, Nacalai Tesque Inc.) was used, with toluene as the mobile phase. The collected fullerenes were purified twice using the same column. The purity of the collected samples was checked by DCI negative-ion mass spectrometry (Finnigan TSQ 7000). The UV-vis absorption spectra of the isolated fullerenes were recorded with a Milton Roy spectrometer (Spectronic 3000). The absolute absorption coefficients of the fullerenes at 0.532 μm were obtained by measuring the light absorption at this wavelength and by carefully weighing the dried fullerene samples in a balance (Autobalance Model AD-6) to get the concentrations.

Since the accuracy in fullerene concentration measurements will directly affect the accuracy of the determination of nonlinear susceptibilities, great care was taken to minimize the measurement uncertainties. The fullerene/ CS_2 sample was carefully injected into a weighed aluminum cup (~ 0.5 mL) with a 0.5 mL syringe. After the solvent evaporated completely, the cup was put into a vacuum desiccator to remove possible water condensed from air. Each sample was evaporated and weighed at least three times. The absolute error for each sample was estimated to be less than 0.002 mg for a 0.5 mL solution, and the relative error for the determination of the concentrations was estimated to be less than 5%.

The DFWM experimental setup has been described previously.^{29,32} Briefly, the experiment was carried out in a counterpropagation geometry. The excitation beam was derived from the 70 ps second-harmonic radiation (0.532 μm) of a CW mode-locked Nd:YAG laser (Coherent, Antares 76-S) with a repetition rate of 500 Hz (Q-switched). Ninety percent of the laser power was evenly split between the two counterpropagating pump pulses with the remaining 10% going to the probe pulse, which was chopped at 250 Hz. The three beams were temporally and spatially overlapped in the sample. The laser beam was vertically polarized, and the angle between the pump and probe beams was $\sim 3^\circ$. The beam diameter was 0.6 mm at the fullerene sample solution contained in a 1 mm thick quartz cell, and the applied peak power density was 6 MW/cm². The phase conjugate signal was detected by a photodiode connected to a lock-in amplifier (SR850 DSP) behind a mirror of 50% reflectivity. Fresh CS_2 was used as a calibration standard for the measurements.

III. Results and Discussion

Figure 1 shows the optical absorption spectra of the series of fullerenes dissolved in CS_2 which were used for the DFWM measurements. The absorption spectra are scaled based on a concentration of 0.1 g/L to facilitate comparison. Some of the absorption spectra have been reported previously by other research groups.^{27,28} Our absorption spectra obtained for C_{60} , C_{70} , C_{76} , C_{78} , C_{84} , C_{90} , and C_{96} are essentially the same as those reported by Kikuchi et al.²⁷ and Diederich et al.,²⁸ indicating the high purity of our fullerene samples. The purity ($>97\%$) of our samples was also checked by HPLC and DCI negative-

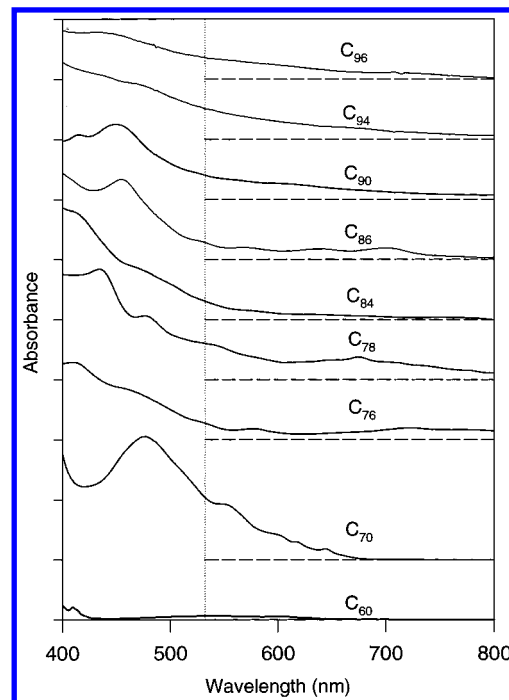


Figure 1. UV-vis absorption spectra of fullerenes in CS_2 . CS_2 was used as a reference. The spectra were normalized to the condition of a fullerene concentration at 0.1 g/L and the light path length 1 cm. The vertical line indicates the excitation wavelength (0.532 μm) for the DFWM measurements.

ion mass spectra.²⁹ To our knowledge, there has been no report on the spectra of C_{86} and C_{94} until this work. As can be seen clearly from Figure 1, the low-energy absorption tail gradually shifts to the red with the increase of the fullerene cage size. This in general reflects the narrowing of the HOMO-LUMO gaps of the fullerenes as the fullerene size increases although the lowest energy electronic transition may not be dipole-allowed for some fullerenes, particularly C_{60} . The excitation wavelength (0.532 μm) for the DFWM measurements is indicated in Figure 1. The absorption coefficients at this wavelength vary depending on the specific fullerenes under study due to their different electronic energy level structures at this excitation energy.

In Figure 2, the dependence of the conjugate signal intensities from three C_{84} solutions of different concentration on the incident laser power is shown. At low concentrations (<0.1 g/L), typical linear correlations in the log-log plot with a slope of ~ 3 can be obtained within the whole incident laser power range we explored, indicating a third-order nonlinear optical process. At higher concentrations of C_{84} (~ 0.1 g/L), however, DFWM signals are saturated at the high end of the incident laser powers (~ 30 mW). This was found to be the case in general for all the fullerenes we have studied. Figure 3, which gives the dependence of the conjugate signal intensities from four C_{70} solutions of different concentration on the incident laser power, shows more clearly that the higher the fullerene concentration, the lower the saturation laser power. This implies that the DFWM signal saturation is likely to be caused by the nonlinear optical absorption (ref 8) since the photoabsorption increases with both the fullerene concentration and the laser power. Saturated conjugation signals from a C_{60}/CS_2 solution were also observed but with a higher concentration (~ 0.5 g/L under 30 mW pump power). At the same incident pump laser power of 30 mW, the dependence of the saturation concentrations on fullerene cage size is shown in Figure 4. The linear absorption coefficients of the fullerene/ CS_2 solutions with a

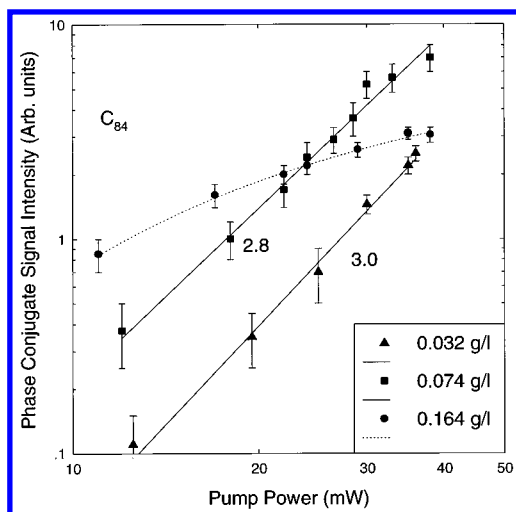


Figure 2. Dependence of the phase conjugate signal intensity on the incident laser intensity measured for different concentrations of C_{84} in CS_2 . The solid lines are linear regressions by fitting to the corresponding data points with slopes indicated by the numbers. The dotted line is drawn by connection of data points at high concentration (0.16 g/L).

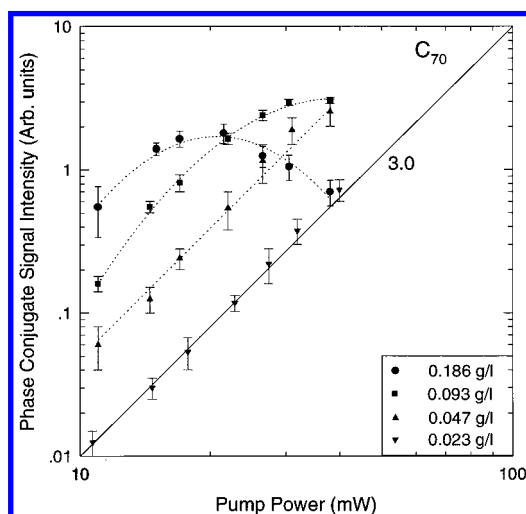


Figure 3. Dependence of the conjugate signal intensity on the incident laser intensity measured for different concentrations of C_{70} in CS_2 . The solid lines are linear regressions by fitting to the corresponding data points. The dotted lines are drawn by connection of data points at high concentrations.

concentration of 0.1 g/L are shown in the same figure. There exists a clear anticorrelation between the linear absorption coefficient and the saturation concentration, which corroborate our above suggestion that nonlinear optical absorption may be an important factor for the DFWM signal saturation.

One particular feature in Figures 2 and 3 is noteworthy. For the relatively concentrated fullerene solutions, instead of leveling off as expected for saturation, the DFWM signal decreases sharply at sufficiently high incident laser powers. Under such a circumstance, a set of cone shells was observed in the sample, which produced concentric rings when projected on a screen. We believe that this phenomenon may be attributable to the photoabsorption-mediated thermal grating effect.^{33–36} To avoid the above situation, the optimum concentrations of higher fullerenes and C_{60} in CS_2 for the nonlinear optical measurements should have an upper limit. On the other hand, the fullerene solutions cannot be too dilute since the signal intensity would then be too weak for determining the third-order nonlinear susceptibilities with a reasonable accuracy. This sets up a lower fullerene concentration limit for the nonlinear optical measure-

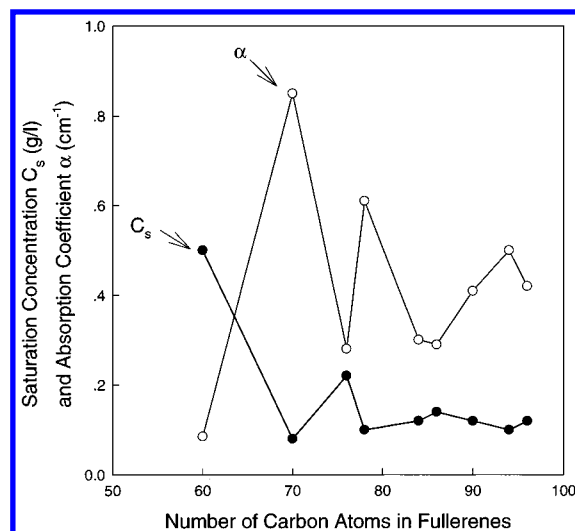


Figure 4. Saturation concentrations and linear absorption coefficients of different fullerenes versus the number of atoms in fullerenes. The solid circles indicate the saturation concentration under the incident pump power 30 mW. The open circles represent the linear absorption coefficients obtained from 0.1 g/L fullerene solutions.

ments. The optimum concentrations were found to be in the range 0.2–0.5 g/L for C_{60} , 0.03–0.2 g/L for C_{76} , and generally 0.02–0.1 g/L for other fullerenes. The optimum single pump laser power was found to be 15–30 mW, which can be optimized further according to the different fullerene samples and their concentrations.

Since there is an appreciable linear absorption at the excitation wavelength ($0.532 \mu\text{m}$) for the fullerene series, we need to take it into account in deriving the third-order susceptibilities from our DFWM measurements. The third-order susceptibilities of the fullerene series were determined according to the following equation:^{5,36}

$$\chi_{1111,S}^{(3)} = \frac{\alpha_S L_S}{e^{-\alpha_S L_S/2}(1 - e^{-\alpha_S L_S})} \left(\frac{I_S}{I_R} \right)^{1/2} \left(\frac{n_S}{n_R} \right)^2 \frac{L_R}{L_S} \chi_{1111,R}^{(3)} \quad (1)$$

where $\chi_{1111,S}^{(3)}$ and $\chi_{1111,R}^{(3)}$ are the third-order optical susceptibility of the sample and the reference, respectively; I_S and I_R are the conjugate signals from the sample and the reference; n_S and n_R are the refractive indices of the sample and the reference; α_S is the linear absorption coefficient of the sample; and L_S and L_R are the interaction lengths of the sample and the reference, respectively.

The values of $\chi^{(3)}$ for the fullerenes were obtained by plugging the measured data into eq 1. As a reference, $\chi_{1111}^{(3)}$ of the pure CS_2 liquid is used, which is 2.3×10^{-13} esu.³⁷ Figure 5 shows $\chi^{(3)}$ of the C_{84}/CS_2 solutions obtained by the above procedure as a function of the fullerene concentration. In this plot, different data points at a given concentration of C_{84} were obtained for different excitation laser power. In our data treatment, we ignored the points represented by small crosses in Figure 5 since these points do not follow the cubic dependence of the phase conjugate signal vs the pump laser power (see Figure 2). By fitting the valid data points into a straight line in Figure 5, we found that the line does not go to zero at zero concentration but has a positive intercept. This suggests that the contribution of the CS_2 solvent to the gross third-order nonlinear susceptibility of the C_{84}/CS_2 solution is not negligible in our DFWM measurements. A similar situation was observed previously for C_{60} and C_{70} in toluene and benzene by other researchers.^{6,38} Since the fullerene solutions under study are

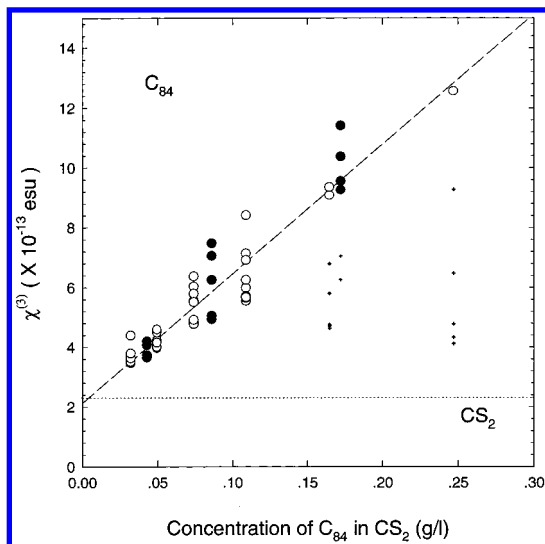


Figure 5. Dependence of $\chi^{(3)}$ of C_{84} on the concentration of C_{84} in CS_2 . The two sets of data indicated by circles (filled and open) were obtained from two completely independent measurements in the range of cubic dependence of the conjugate signals on the incident laser powers. The points represented by small crosses are out of the cubic range and are therefore not included in the line fitting.

in general quite dilute, we can assume that the dissolved fullerene molecules are noninteracting constituents so that a pairwise additive model¹⁵ can be used to derive the true nonlinear susceptibilities of fullerenes. In this model, $\chi_{1111}^{(3)}$ of the fullerene solution equals approximately to the linear combination of $\chi_{1111}^{(3)}$ of the solvent and that of the solute. Therefore, the contribution of the CS_2 solvent was accounted for by subtracting $\chi_{1111}^{(3)}$ of pure CS_2 from $\chi_{1111}^{(3)}$ of the fullerene/ CS_2 solution.

To assess the intrinsic nonlinear optical properties of fullerenes, we normalize the third-order optical nonlinearity to a single molecule. This is done through the relation $\gamma_{1111} = \chi_{1111}^{(3)}/NL^4$, where γ_{1111} is the second hyperpolarizability, N is the number of molecules per unit volume, and L is the Lorentz field factor. The Lorentz field factor is given by $L = [(n^2 + 2)/3]$, where n is the refractive index. From the set of $\chi_{1111}^{(3)}$ values, the second hyperpolarizabilities of fullerenes are determined through a statistical analysis in which 3 times the standard deviation ($\pm 3\sigma$) was taken for the uncertainty of measured γ_{1111} . The result for the γ_{1111} of C_{84} obtained following the above procedure is shown in Figure 6. From this figure, it may seem that the γ_{1111} values of C_{84} from our measurements are radically scattered at first glance. It should be noticed, however, that the data points represented by small crosses should be ignored in our analysis since these points are outside the phase conjugate signal—laser power cubic dependence range. After eliminating these data points, our measurements are more consistent among each other although a certain degree of scatter still exists. The relatively large variation of γ_{1111} from DFWM measurements is not unusual and is due to the high sensitivity of a third-order nonlinear optical response to the excitation laser power. Nevertheless, the statistical analysis should give a reasonably accurate estimate of γ_{1111} . In the case of C_{84} , γ_{1111} is estimated to be $(1.2 \pm 0.3) \times 10^{-30}$ esu as shown by the broken line in Figure 6.

Table 1 summarizes the linear and nonlinear optical properties of the fullerenes obtained from our experiments. Although relatively large error bars are involved for the data of $\chi^{(3)}$ and γ_{1111} , one can still identify the differences of the $\chi^{(3)}$ or γ_{1111} among different fullerenes. In general, the second hyperpolar-

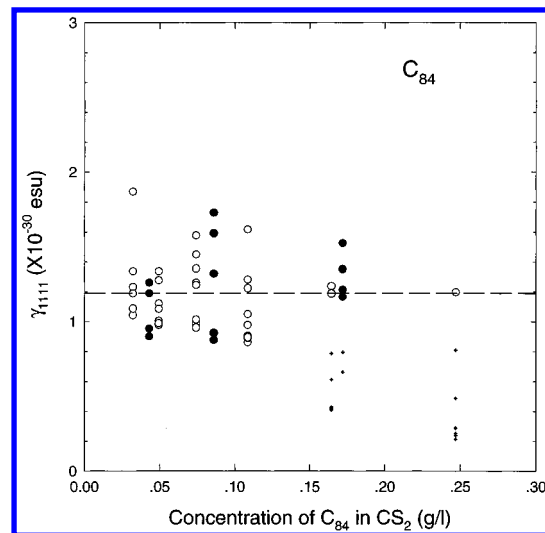


Figure 6. Plot of the measured second hyperpolarizabilities γ_{1111} of C_{84} dissolved in CS_2 as a function of concentrations. The meanings of the symbols are the same as those in Figure 5.

izabilities γ_{1111} of all these fullerenes were determined to be on the order of 10^{-31} – 10^{-30} esu. In addition, there exists an apparent global trend that higher fullerenes show larger nonlinear optical responses. This can be better appreciated from Figure 7, which shows the dependence of γ_{1111} on the number of carbon atoms in fullerenes. Aside from the general trend mentioned above, Figure 7 reveals that the γ_{1111} of C_{70} and C_{78} exhibit prominent enhancement compared to those of their neighboring fullerenes.

It is generally believed that the large optical response of fullerenes originates from transient motion of the π -conjugated electrons occurring upon the laser excitation. Since there are more highly delocalized π -conjugated electrons over the spherical-like surface in higher fullerenes compared to C_{60} , the larger γ_{1111} of high fullerenes are expected. According to the model of free-electron gas confined in a spherical shell and the sum of states calculations,^{17,22} the optical nonlinearity scales with the third power or fourth power of the number of carbon atoms. We are now in a position for the first time to compare the theory with our experiment regarding the nonlinear optical properties as a function of the fullerene cage size. This is shown in Figure 7 plotted in a log–log scale. The general increase, in particular the cubic to quartic dependence, in the third-order susceptibilities of the fullerenes from C_{60} to C_{96} is certainly consistent with the trend of the theoretical prediction. However, the theoretical prediction of γ is about 4 orders of magnitude less than our experimental results. In addition, the γ_{1111} of C_{70} and C_{78} display clearly anomalously higher second hyperpolarizabilities. These suggest that other contributing factors such as molecular structure and resonance enhancement to the increased second hyperpolarizability may be important as well. Indeed, these two fullerenes do show enhanced linear absorptions at the excitation laser wavelength as shown in Figure 1.

Studies on conjugated polymeric nonlinear optical materials in the past revealed the high nonlinear susceptibilities of linear conjugated structures. Such a molecular structural effect on the nonlinear optical properties may also be present in the fullerene materials. Among the fullerenes, the I_h symmetry of C_{60} probably makes it more difficult to be polarized than the less spherical structures of higher fullerenes, which could be one of the reasons for the smaller γ_{1111} of C_{60} . The nonlinear susceptibility of a fullerene molecule can be phenomenologically related to a length–diameter ratio of the carbon cage. Since

TABLE 1: Linear and Nonlinear Optical Properties of Fullerenes^a

	C ₆₀	C ₇₀	C ₇₆	C ₇₈	C ₈₄	C ₈₆	C ₉₀	C ₉₄	C ₉₆
α (cm ⁻¹)	0.086	0.85	0.28	0.61	0.30	0.29	0.41	0.50	0.42
$\chi^{(3)}$ (10 ⁻¹³ esu)	1.0 ± 0.3	4.3 ± 1.4	2.8 ± 1.0	5.5 ± 1.0	3.9 ± 1.0	4.9 ± 1.5	7.2 ± 2.0	6.0 ± 2.0	6.7 ± 2.0
γ_{1111} (10 ⁻³⁰ esu)	0.22 ± 0.06	1.3 ± 0.4	0.8 ± 0.3	1.5 ± 0.3	1.2 ± 0.3	1.3 ± 0.5	1.8 ± 0.6	1.9 ± 0.6	2.1 ± 0.6
$\chi^{(3)}/\alpha$ (10 ⁻¹³ esu cm ⁻¹)	11 ± 3	5 ± 2	10 ± 3	9 ± 2	13 ± 2	17 ± 3	17 ± 4	12 ± 4	16 ± 4

^a α and $\chi^{(3)}$ were normalized to the concentration at 1.0 g/L.

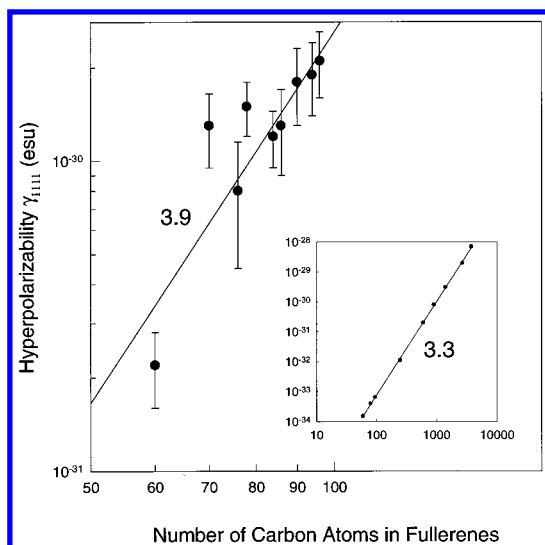


Figure 7. Measured second hyperpolarizabilities γ_{1111} versus the number of carbon atoms in the fullerene molecules. The plot in the inset shows the theoretical prediction.^{17,22} The numerical figures (3.9 and 3.3) indicate the slopes of the corresponding solid lines.

the length–diameter ratios of C₇₀ (*D*_{5h}) and C₇₈ (*C*_{2v} and *D*₃) are higher than that of C₇₆ (*D*₂) according to the ¹³C NMR studies by Diederich et al.,²⁸ this argument may be taken to account for the prominent nonlinear optical response of these two fullerenes as can be seen in Figure 7. There are many more possible isomers for even higher fullerenes though with the constraints of Euler’s rule and the isolated pentagon rule, the number of possible fullerene structures of a given C_n is reduced considerably. It was found numerically that there are 24 for C₈₄, 46 for C₉₀, and 187 for C₉₆.^{39,40} Further separation of different higher fullerene isomers was not carried out in the present work. Electrochemistry⁴¹ and ¹³C NMR^{28,42} studies suggested that *D*₂ and *D*_{2d} were the two most abundant structures for C₈₄. The theoretical studies^{40,43,44} found a *C*₂ isomer to be the most stable C₉₀ and a *D*₂ isomer for C₉₆, while UPS studies⁴⁵ suggested a *C*₁ geometry to be the first candidate for the main isomer of C₉₆. Much less information is available regarding the isomers of other higher fullerenes. Since the second hyperpolarizabilities of the higher fullerenes (from C₈₄ to C₉₆) increase smoothly, it appears that these fullerenes do not exhibit dramatic differences in the length-to-diameter ratio.

To fully understand the differences of nonlinear optical responses among the fullerene series under study, resonance enhancement should be considered since there exists an appreciable absorption at the laser excitation wavelength of 0.532 μ m (see Figure 1). From Figure 1 and Table 1, we can appreciate that the absorption coefficients (α) of C₇₀ and C₇₈ are larger than that of other higher fullerenes. This can also partially explain the exceptionally larger γ_{1111} of these two fullerenes. Therefore, the trend of second hyperpolarizability of fullerenes will be the tradeoff among the number of π -conjugated electrons over fullerene cages, geometrical structure of fullerene molecule, and resonance enhancement effect.

The third-order nonlinear optical properties of the fullerene

materials can be further characterized by a figure of merit, $\chi^{(3)}/\alpha$, which is used to appraise the applicability of the materials in nonlinear optics. The figures of merit of the fullerenes are also tabulated on the last row in Table 1. Although $\chi^{(3)}/\alpha$ as a function of the fullerene cage size exhibits much less regularity than for γ_{1111} or $\chi^{(3)}$, globally, it still increases with the cage size. The figures of merit of the fullerenes we have studied are comparable with or even larger than those of transition-metal oxides which were recently found to possess large optical nonlinearities.⁴⁶ Of all the fullerenes we have studied, C₈₆ and C₉₀ show the largest figures of merits. Among all the empty fullerenes we have studied so far, however, the most abundant and highly symmetrical C₆₀ still appears to be the molecule of choice for the third-order nonlinear optical applications at the laser excitation wavelength (0.532 μ m) due to its relatively high $\chi^{(3)}/\alpha$ and availability. Nevertheless, we want to point out that the figure of merit is expected to increase with the fullerene cage size. The consequence is that the extremely large fullerenes—carbon nanotubes with their large aspect ratio (an essentially one-dimensional structure) and their superextensive π -electron conjugation—are likely to be a potential candidate as a future nonlinear optical material.

IV. Summary and Conclusions

In summary, we showed through the DFWM measurements that the fullerene series from C₆₀ to C₉₆ shows a large third-order nonlinear optical response at 0.532 μ m. The concentrations of fullerenes and the incident laser powers were found to be vitally important in the DFWM measurements and are therefore optimized. The second hyperpolarizabilities of these fullerenes were determined to be on the order of 10⁻³¹–10⁻³⁰ esu, in which exists a trend that higher fullerenes show larger γ_{1111} . The reasons for the trend were discussed based on the model of a free-electron gas confined in a spherical shell and the distortion-enhanced and resonance-enhanced third-order optical nonlinearity.

Acknowledgment. This work was supported by an HIA grant of HKUST and an RGC Grant (HKUST601/95P) administered by the UGC of Hong Kong. G. Gu thanks the Chinese NSF for the support. The nonlinear optical measurements were carried out in the Joyce M. Kuok Lasers and Photonics Laboratory of the Advanced Materials Institute at HKUST. J. Fu and P. Yu gratefully acknowledge the financial support provided by the Hong Kong Telecom Institute of Information Technology.

References and Notes

- (1) Blau, W. J.; Byrne, H. J.; Cardin, D. J.; Dennis, T. J.; Hare, J. P.; Kroto, H. W.; Taylor, R.; Malton, D. R. M. *Phys. Rev. Lett.* **1991**, *67*, 1423.
- (2) Hoshi, H.; Nakamura, N.; Maruyama, Y.; Nakagawa, T.; Suzuki, S.; Shiromaru, H.; Achiba, Y. *Jpn. J. Appl. Phys.* **1991**, *30*, L1397.
- (3) Wang, Y.; Cheng, L. *J. Phys. Chem.* **1992**, *96*, 1530.
- (4) Gong, Q.; Sun, Y.; Xia, Z.; Zou, Y. H.; Gu, Z.; Zhou, X.; Qiang, D. *J. Appl. Phys.* **1992**, *71*, 3025.
- (5) Kafafi, Z. H.; Lindle, J. R.; Pong, R. G. S.; Bartoli, F. J.; Lingg, L. J.; Milliken, *Chem. Phys. Lett.* **1992**, *188*, 492.

- (6) Zhang, Z.; Wang, D.; Ye, P.; Li, Y.; Wu, P.; Zhu, D. *Opt. Lett.* **1992**, *17*, 973.
- (7) Talapatra, G. B.; Manickam, N.; Samoc, M.; Orczyk, M. E.; Karna, S. P.; Prasad, P. N. *J. Phys. Chem.* **1992**, *96*, 5206.
- (8) Tutt, L. W.; Kost, A. *Nature* **1992**, *356*, 225. Gu, G.; Zhang, W.; Zen, H.; Du, Y.; Han, Y.; Zhang, W.; Dong, F.; Xia, Y. *J. Phys. B* **1993**, *26*, L451.
- (9) Rosker, M. J.; Marcy, H. O.; Chang, T. Y.; Khoury, J. T.; Hansen K.; Whetten, R. L. *Chem. Phys. Lett.* **1992**, *196*, 427.
- (10) Neher, D.; Stegeman, G. I.; Tinker, F. A.; Peyghambarian, N. *Opt. Lett.* **1992**, *17*, 1491.
- (11) Vijaya, R.; Murti, Y. V. G. S.; Sundararajan, G.; Mathews, C. K.; Rao, P. R. V. *Opt. Commun.* **1992**, *94*, 353.
- (12) Henari, F.; Callaghan, J.; Stiel, H.; Blau, W.; Cardin, D. J. *Chem. Phys. Lett.* **1992**, *199*, 144.
- (13) Aranda, F. J.; Rao, D. V. G. L. N.; Roach, J. F.; Tayebati, P. J. *Appl. Phys.* **1993**, *73*, 7949.
- (14) Kost, A.; Tutt, L.; Klein, M. B.; Dougherty, T. K.; Elias, W. E. *Opt. Lett.* **1993**, *18*, 334.
- (15) Tang, N.; Partanen, J. P.; Hellwarth, R. W.; Knize, R. J. *Phys. Rev. B* **1993**, *48*, 8404.
- (16) Ji, W.; Tang, S. H.; Xu, G. Q.; Chan, H. S. O.; Ng, S. C.; Ng, W. W. *J. Appl. Phys.* **1993**, *74*, 3669.
- (17) Knize, R. J. *Opt. Commun.* **1994**, *106*, 95.
- (18) Kajzar, F.; Taliani, C.; Danieli, R.; Rossini, S.; Zamboni, R. *Chem. Phys. Lett.* **1994**, *217*, 418.
- (19) Zhou, D.; Gan, L.; Luo, C.; Tan, H.; Huang, C.; Liu, Z.; Wu, Z.; Zhao, X.; Xia, X.; Zhang, S.; Sun, F.; Xia, Z.; Zou, Y. *Chem. Phys. Lett.* **1995**, *235*, 548.
- (20) Yang, L.; Royer, E.; Walser, A. D.; Dorsinville, R. *Chem. Phys. Lett.* **1995**, *239*, 399.
- (21) Sun, F.; Zhang, S.; Xia, Z.; Zou, Y. H.; Chen, X.; Qiang, D.; Zhou, X.; Wu, Y. *Phys. Rev. B* **1995**, *51*, 4614.
- (22) Fanti, M.; Orlandi, G.; Zerbetto, F. *J. Am. Chem. Soc.* **1995**, *117*, 6101.
- (23) Xu, Q.; Dong, J.; Jiang, J.; Xing, D. Y. *J. Phys. B: At. Mol. Opt. Phys.* **1996**, *29*, 1563.
- (24) Geng, L.; Wright, J. C. *Chem. Phys. Lett.* **1996**, *248*, 105.
- (25) Moore, C. E.; Cardelino, B. H.; Wang, X. Q. *J. Phys. Chem.* **1996**, *100*, 4685.
- (26) Kajzar, F.; Taliani, C.; Zamboni, R.; Rossini, S.; Danieli, R. *Synth. Met.* **1996**, *77*, 257.
- (27) Kikuchi, K.; Nakahara, N.; Wakabayashi, T.; Honda, M.; Matsumiya, H.; Moriwaki, T.; Suzuki, S.; Shiromaru, H.; Saito, K.; Yamauchi, K.; Ikemoto, I.; Achiba, Y. *Chem. Phys. Lett.* **1992**, *188*, 177.
- (28) Diederich, F.; Whetten, R. L. *Acc. Chem. Res.* **1992**, *25*, 119.
- (29) Huang, H. J.; Gu, G.; Yang, S. H.; Fu, J. S.; Yu, P.; Wong, G. K. L.; Du, Y. W. *Chem. Phys. Lett.* **1997**, *272*, 427.
- (30) Ding, J. Q.; Weng, L. T.; Yang, S. H. *J. Phys. Chem.* **1996**, *100*, 11120.
- (31) Ding, J. Q.; Yang, S. H. *Angew. Chem., Int. Ed. Engl.* **1996**, *35*, 2234.
- (32) Liao, H. B.; Xiao, R. F.; Fu, J. S.; Yu, P.; Wong, G. K. L.; Sheng, P. *Appl. Phys. Lett.* **1997**, *70*, 1.
- (33) Zyss, J. *Molecular Nonlinear Optics*; Academic Press: New York, 1994.
- (34) Woggon, U. *Optical Properties of Semiconductor Quantum Dots*; Springer-Verlag Press: Berlin, 1997.
- (35) Qian, S.; Song, J.; Wang, G.; Li, Y. *Nonlinear Optics: Materials, Fundamentals and Applications Technical Digest*; Optical Society of America: Washington, DC, 1992.
- (36) Prasad, P. N.; Williams, D. J. *Introduction to Nonlinear Optical Effects in Molecules and Polymers*; Wiley-Interscience: New York, 1991.
- (37) Meredith, G. R.; Buchalter, B.; Hanzlik, C. *J. Chem. Phys.* **1983**, *78*, 1543.
- (38) Kafafi, Z. H.; Bartoli, F. J.; Lindle, J. R.; Pong, R. G. S. *Phys. Rev. Lett.* **1992**, *68*, 2705.
- (39) Fowler, P. W. *J. Chem. Soc., Faraday Trans.* **1991**, *87*, 1945.
- (40) Murry, R. L.; Scuseria, G. E. *J. Phys. Chem.* **1994**, *98*, 4212.
- (41) Yang, Y.; Arias, F.; Echegoyen, L.; Chibante, L. P. F.; Flanagan, S.; Robertson, A.; Wilson, L. J. *J. Am. Chem. Soc.* **1995**, *117*, 7801.
- (42) Schneider, U.; Richard, S.; Kappes, M. M.; Ahlrichs, R. *Chem. Phys. Lett.* **1993**, *210*, 165.
- (43) Zhang, B. L.; Wang, C. Z.; Ho, K. M.; Xu, C. H.; Chan, C. T. *J. Chem. Phys.* **1993**, *9*, 3095.
- (44) Liu, X.; Schmalz, T. G.; Klein, D. J. *Chem. Phys. Lett.* **1992**, *188*, 550.
- (45) Hino, S.; Takahashi, H.; Iwasaki, K.; Miyazaki, T.; Kikuchi, K.; Achiba, Y. *Chem. Phys. Lett.* **1994**, *230*, 165.
- (46) Ando, M.; Kadono, K.; Haruta, M.; Sakaguchi, T.; Miya, M. *Nature* **1995**, *374*, 625.